Tumor-wide RNA splicing aberrations generate immunogenic public neoantigens across cancers

Darwin Kwok[1], Nicholas Stevers[1], Inaki Etxeberria[2,3], Takahide Nejo[1], Maggie Colton Cove[1], Lee H Chen[1], Jangham Jung[1], Kaori Okada[1], Senthilnath Lakshmanachetty[1], Marco Gallus[1], Abhilash Barpanda[4], Chibo Hong[1], Gary KL Chan[1], Jerry Liu[1], Samuel H Wu[1], Emilio Ramos[4], Akane Yamamichi[1], Payal Watchmaker[1], Hirokazu Ogino[1], Atsuro Saijo[1], Aidan Du[1], Nadia Grishanina[1], James Woo[1], Aaron Diaz[1], Susan M Chang[1], Joanna J Phillips[1,5], Arun Wiita[4,5,6], Christopher Klebanoff[2,3,8], Joseph Costello[1], Hideho Okada[1,8]

[1]Department of Neurological Surgery, University of California, San Francisco, San Francisco, CA, United States [2]Human Oncology and Pathogenesis Program (HOPP), Immuno-Oncology Service, Memorial Sloan Kettering Cancer Center, New York, NY, United States [3]Parker Institute for Cancer Immunotherapy, New York, NY, USA [4]Department of Laboratory Medicine, University of California, San Francisco, San Francisco, CA, United States [5]Department of Bioengineering and Therapeutic Sciences, University of California, San Francisco, CA, United States [6]Chan Zuckerberg Biohub San Francisco, San Francisco, CA, United States [7]Department of Pathology, San Francisco, CA, University of California, San Francisco, San Francisco, CA, United States [8]Department of Medicine, Memorial Sloan Kettering Cancer Center, New York, NY, United States [9]Parker Institute for Cancer Immunotherapy, San Francisco, San Francisco, CA, United States

Weill Institute for Neurosciences

Helen Diller Family Comprehensive Cancer Center

BACKGROUND

Cell-based immunotherapy shows durable survival benefits in various cancers.[1-2] Yet, many tumors evade eradication due to intratumoral heterogeneity (ITH)[3-7] of their cellular and genetic landscape. Despite immunotherapeutic success in cancers with high immune infiltration and mutational load,[8] cancers with extensive ITH or lower mutational burdens are more resistant.[9-11] Current strategies targeting tumor-specific antigens (TSAs) focus on peptides that arise from somatic nonsynonymous mutations,[12] however this approach yields limited targets in tumors with low mutational burdens.[13] To expand the repertoire of potential immunotherapeutic antigens, recent studies explored cancer-specific splicing events, otherwise known as neojunctions (NJs), as a source of TSAs. Nevertheless, no study has examined the spatial and temporal conservation of NJs across whole tumors. Thus, whether neojunction-derived targets are clonally conserved remains unknown.

To address this clinically relevant knowledge gap, we investigated the clonality of neojunctions across cancer types to identify shared, or “public”, tumor-wide NJ-derived TSAs. We developed the Spatial Splicing Neoantigen Identifier Pipeline (SSNIP) for characterizing NJs found across multiple intratumoral sites (spatially-conserved) by systematically mapping NJs across distinct regions in the same tumor. **(Figure 1)** We identified immunogenic NJ-derived TSAs proteolytically-processed and presented on prevalent human leukocyte antigen (HLA) molecule. Recognition of these antigens by TSA-specific CD8+ T-cells induced T-cell receptor (TCR) signaling and antigen-dependent tumor cell killing. Together, these findings highlight the potential of targeting tumor-wide public NJ-derived TSAs as a novel class of “off-the-shelf” cancer immunotherapies, offering a promising avenue for improving cancer treatments.

IDENTIFICATION OF NEOJUNCTIONS IN TUMORS

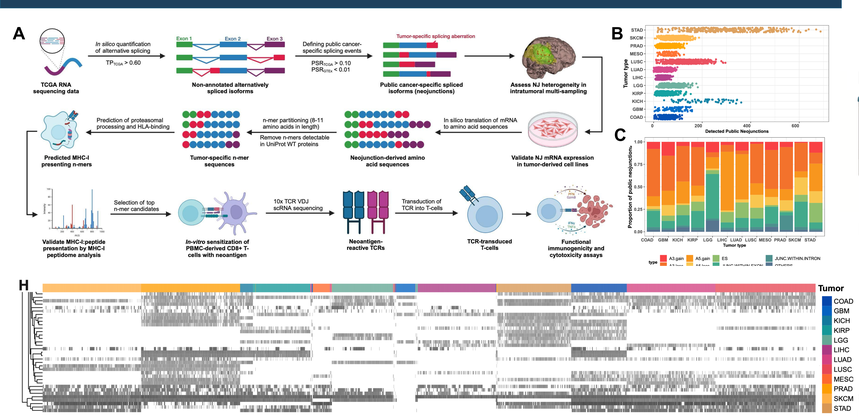

Figure 1: Identification of neojunctions (NJs) in TCGA samples. A. Pipeline for identifying putative, tumor-wide, cancer-specific alternative splicing events from RNA-sequencing data from The Cancer Genome Atlas (TCGA) **B.** Total public neojunctions detected per sample across tumor types **C.** Distribution of public neojunctions based on splice types: exonic loss due at the 3’ or 5’ splice site (A3 or A5 loss), intronic gain at the 3’ or 5’ splice site (A3 or A5 gain), exon skip (ES), junction within exon, junction within intron, others (**F**) and frame-shift (fs) status **D.** Expression of all pan-cancer-spanning neojunctions (log_2(CPM)) across all studied TCGA tumor types.

NJ INTRATUMORAL HETEROGENEITY ACROSS CANCER TYPES

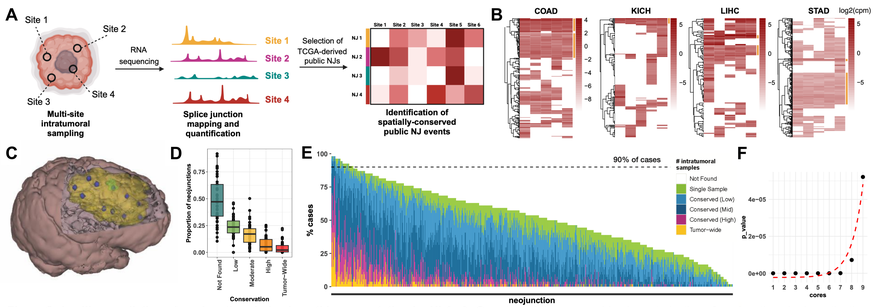

Figure 2: *in silico* prediction of neojunction-derived peptide presentation by HLA. A. Overview of the tumor-wide characterization of neojunctions by investigating RNA-sequencing of multiple intratumoral regions in various cancer types. **B.** Heatmaps representing log_2(CPM) of neojunctions (rows) across five samples within the same tumor (columns) in colon adenocarcinoma (COAD), kidney chromophobe (KICH), liver cancer (LIHC), and stomach adenocarcinoma (STAD). Neojunctions found across all five intratumoral samples are annotated in yellow. **C.** 3-D model of the brain and tumor (yellow) derived from patient 470 (P470). Approximately 10 spatially mapped and maximally distanced biopsies (blue) were taken within each. Whole-exome sequencing, RNA-sequencing, and further analyses were conducted on samples each of these regions. **D.** Box and whisker plots of glioma-specific neojunctions (*n*=789) based on their ITH across patients. **E.** Distribution of glioma-specific neojunctions (*n*=789, columns) based on their ITH across patients. **F.** Dot-plot with best-fitting curve mapping the p-values of all paired *n* core and 10 core iterations.

NJ-SPECIFIC TCRS ARE IDENTIFIED FROM DONOR-DERIVED PBMCS

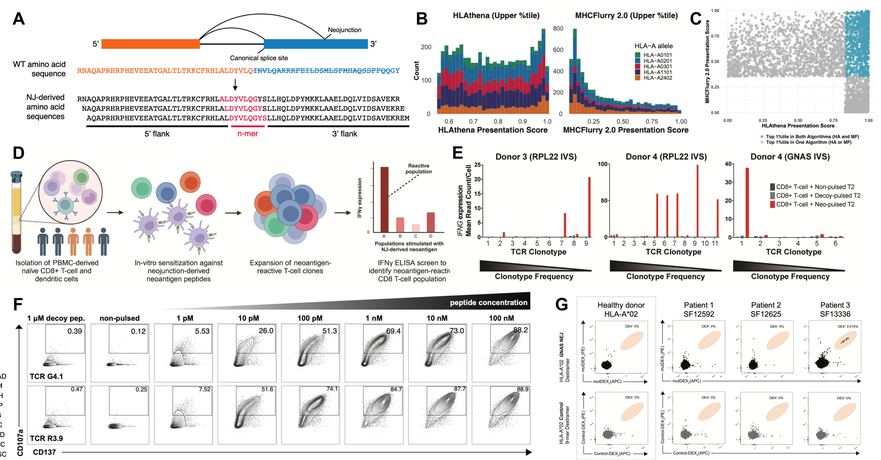

Figure 3: NJ-specific TCRs are identified from donor PBMCs. A. Schematic demonstrating the selection of high-confidence neojunctions for downstream analysis. **B.** Histogram illustrating the scores pertaining to the likelihood of peptide presentation calculated from each algorithm for the top scoring 1-percentile of n-mers categorized by HLA-allele. **C.** Composite presentation scores of the final candidate list of top scoring n-mers that are also validated as detected in RNA-sequencing and mass spectrometry data. **D.** Pipeline overview for identifying neojunction-derived neoantigen-reactive T-cell populations through *in vitro* sensitization (IVS). **E.** 10x V(D)J *IFNG* signatures of highly proliferated TCR clonotypes cultured against T2 cells pulsed with the neoantigen (colored), a control peptide (light-gray), or no peptide (dark-gray). **F.** $NeoA_{GNAS}$ (top) and $NeoA_{RPL22}$-specific (bottom) TCR-transduced PBMC-derived CD8+ T-cells were activated against neoantigen-pulsed T2 cells in a dose-dependent manner. **G.** $NeoA_{GNAS}$-dextramer staining of bulk CD8+ T-cells derived from an HLA-A*02:01 healthy donor (left) and glioma patients (right).

NJ-DERIVED PEPTIDES ELICIT CD8+ T-CELL RESPONSE

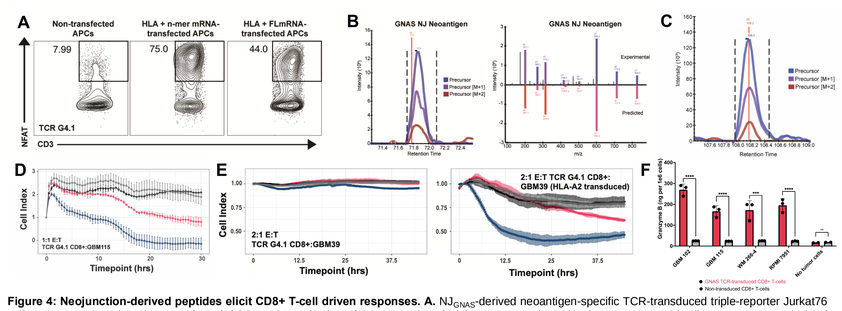

Figure 4: Neojunction-derived peptides elicit CD8+ T-cell driven responses. A. NJ_{GNAS}-derived neoantigen-specific TCR-transduced triple-reporter Jurkat76 cells were co-cultured against transfected COS7. TCR activation of TCR-transduced triple-reporter Jurkat76/CD8 was measured by flow cytometry analysis of NFAT-GFP. **B-C.** Mass spectrometry spectra of NJ_{GNAS}-derived neoantigen n-mers detected through IP-MS/MS following HLA-A*02:01 pulldown of HLA-A*02:01 and full-length neojunction-encoding mRNA-transduced COS7 cells **(B)** and GBM115 tumor cells **(C)**. **D.** NJ_{GNAS}-derived (colored) neoantigen-specific TCR-transduced, or non-transduced (gray) CD8+ T-cells were cultured against GBM115. TCR-transduced CD8+ T-cells were either cultured with GBM115 cells that were non-pulsed (red) or pulsed with 0.1 µM neoantigen peptide. **E.** NJ_{GNAS}-derived neoantigen-specific TCR-transduced CD8+ T-cells cultured with HLA-A2-negative GBM39 cells (left) or HLA-A2-transduced GBM39 cells (right). GBM39 express detectable levels of NJ_{GNAS}. **F.** ELISA readout of secreted Granzyme B by NJ_{GNAS}-TCR-transduced (purple) or non-transduced (gray) CD8+ T-cells when cultured with tumor cell lines.

TUMOR-SPECIFIC SPLICING FACTOR DYSREGULATION GENERATES NJS

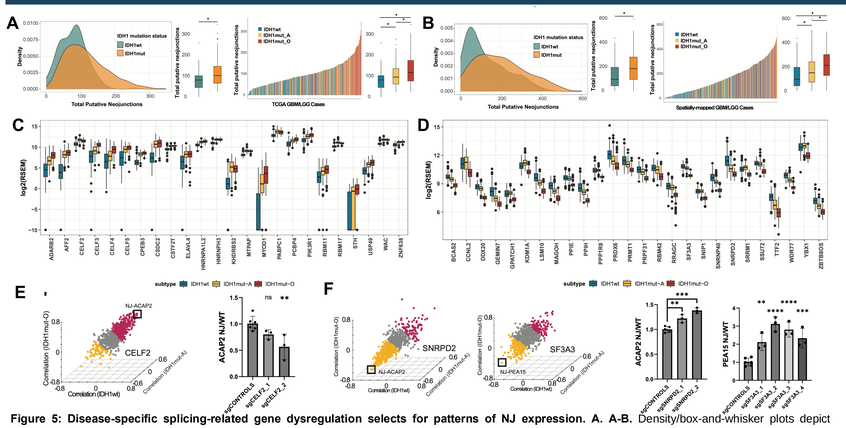

Figure 5: Disease-specific splicing-related gene dysregulation selects for patterns of NJ expression. A. A-B. Density/box-and-whisker plots depict putative neojunctions expressed in *IDH*mut cases (orange) and *IDH*wt cases (green) in TCGA GBM/LGG samples (**A**) and our spatially-mapped GBM/LGG dataset (**B**). **C-D.** Box-and-whisker plot depicting the log_2(RSEM) expression level of IDHmut-specific **(C)** or chromosomes 1p/19q-specific **(D)** splicing-related genes detected from GOBP gene set with a significant ($p < 0.05$) log_2fold increase in expression of 1.5 between *IDH*mut-A (yellow) and *IDH*mut-O (red) cases when compared to *IDH*wt cases (blue). **E-F.** Pearson correlation analyses of glioma-specific neojunctions against the expression of *CELF2*, *SNRPD2*, and *SF3A3* in *IDH*mut-O (z-axis), *IDH*mut-A (y-axis), and *IDH*wt (x-axis) cases, with NJ_{ACAP2} or NJ_{PEA15} boxed. NJs with a Pearson correlation greater than or equal to 0.10 with the corresponding gene are purple and those with a Pearson correlation less than or equal to -0.10 are denoted with yellow dots.

CONCLUSIONS

- Novel integrative *in silico* pipeline identified public, tumor-wide neojunctions.
- 3-D spatial sample analysis revealed neojunctions expressed tumor-wide.
- Neojunction-derived neoepitopes elicited a robust CD8+ T-cell response.

Funding sources:

Dabbiere family, Brain Tumor Funders’ Collaborative, R01CA244838
NIH-supported Predoctoral Training in the Biomedical Sciences, T32GM008568
NCI 2P50CA097257, Brain Tumor Funders' Collaborative,
NCI R01CA244838 R35NS105068 and R01CA222965
Gianne Rae Meadows Grant Award for Oligodendroglioma Cure, ARCS Fellowship Award

References:

1. Ott, P.A. et al. (Nature 2017) “An immunogenic personal neoantigen vaccine for patients with melanoma.”
2. Scholler, J. et al. (Sci. Transl. Med., 2012) “Decade-long safety and function of retroviral-modified chimeric antigen receptor T-cells.”
3. Tirosh, I. et al. (Nature 2016) “Single-cell RNA-seq supports a developmental hierarchy in human oligodendroglioma.”
4. Nicholson, J.G. et al. (Cancer Discov. 2021) “Diffuse glioma heterogeneity and its therapeutic implications.”
5. Teixeira, V.H. et al. (Nat. Med. 2019) “Deciphering the genomic, epigenomic, and transcriptomic landscapes of pre-invasive lung cancer lesions.”
6. Van Galen, P. et al. (Cell 2019) “Single-cell RNA-seq reveals AML hierarchies relevant to disease progression and immunity.”
7. Grosselin, K. et al. (Nat. Genet. 2019) “High-throughput single-cell ChIP-sep identifies heterogeneity of chromatin states in breast cancer.”
8. Samstein, R.M. et al. (Nat. Genet. 2019) “Tumor mutational load predicts survival after immunotherapy across multiple cancer types.”
9. Touat, M. et al. (Nature, 2020) “Mechanisms and therapeutic implications of hypermutation in gliomas.”
10. Russo, M. et al. (Science, 2019) “Adaptive mutability of colorectal cancers in response to targeted therapies.”
11. Huang, Y. et al. (Oncol. Let. 2018) “Molecular and cellular mechanisms of castration resistant prostate cancer.”
12. Stronen, E. et al. (Science 2016) “Targeting of cancer neoantigens with donor-derived T cell receptor repertoires.”
13. Klebanoff, C. et al. (Nat. Med. 2016) “Prospects for gene-engineered T cell immunotherapy for solid cancers.”
14. Kahles, A. et al. (Cancer Cell, 2018) “Comprehensive analysis of alternative splicing across tumors from 8,705 patients.”